

Activation of the (Trimethylsilyl)tetramethylcyclopentadienyl Ligand in Zirconocene Complexes

Michal Horáček,[†] Petr Štěpnička,[‡] Jiří Kubišta,[†] Karla Fejfarová,[‡]
Róbert Gyepes,[‡] and Karel Mach*[†]

*J. Heyrovský Institute of Physical Chemistry, Academy of Sciences of the Czech Republic,
Dolejškova 3, 182 23 Prague 8, Czech Republic, and Department of Inorganic Chemistry,
Charles University, Hlavova 2030, 128 40 Prague 2, Czech Republic*

Received October 23, 2002

Reduction of $[\text{ZrCl}_2\{\eta^5\text{-C}_5\text{Me}_4(\text{SiMe}_3)\}_2]$ (**1**) with excess magnesium in tetrahydrofuran affords a mixture of the monomeric zirconocene hydride $[\text{ZrH}\{\eta^1:\eta^5\text{-C}_5\text{Me}_4(\text{SiMe}_2\text{CH}_2)\}\{\eta^5\text{-C}_5\text{Me}_4(\text{SiMe}_3)\}]$ (**2**) and the dimeric, tetranuclear Zr(III)– and Zr(IV)–magnesium hydride complexes **3** and **4**, respectively. In the presence of bis(trimethylsilyl)ethyne (btmse), a similar reduction yields the η^2 -alkyne complex $[\text{Zr}\{\eta^5\text{-C}_5\text{Me}_4(\text{SiMe}_3)\}_2(\eta^2\text{-btmse})]$ (**5**) as the major product and compounds **2**–**4** as minor impurities. Upon thermolysis under vacuum, **5** undergoes a 2-fold hydrogen transfer from trimethylsilyl groups in the zirconocene intermediate to leaving btmse to afford $[\text{Zr}\{\eta^5:\eta^1\text{-C}_5\text{Me}_4(\text{SiMe}_2\text{CH}_2)\}_2]$ (**6**) and a mixture of alkenes (*E*)- and (*Z*)- $\text{Me}_3\text{SiCH}=\text{CHSiMe}_3$ (*E* \gg *Z*). Crystal structures of compounds **2** and **4**–**6** were determined by X-ray crystallography.

Introduction

The reactivity and catalytic activity of group 4 metallocene complexes in the polymerization of alkenes¹ and other C–C bond-forming reactions² is controlled both by acidity of the active metal center and its spatial accessibility for the reactants.³ These properties can be finely tuned by stepwise substitution of protons at the cyclopentadienyl ring(s). Steric and electronic effects of the most often used substituent, the methyl group, are well established: electron density at the metal generally increases with an increasing number of methyl groups

at the cyclopentadienyl ligands. In the methyl-substituted zirconocene dihalides $[\text{ZrL}_2(\eta^5\text{-C}_5\text{H}_{5-n}\text{Me}_n)_2]$ (*L* = F, Cl, Br; *n* = 0–5) such a relationship was demonstrated by shifts of the electrochemical reduction⁴ and oxidation potentials,⁵ the binding energies of the inner shell electrons,⁵ ⁹¹Zr NMR chemical shifts,⁶ and in $[\text{Zr}(\eta^5\text{-C}_5\text{H}_{5-n}\text{Me}_n)_2(\eta^2\text{-Me}_3\text{SiC}\equiv\text{C}/\text{SiMe}_3)]$ (*n* = 0–5) also by ¹³C NMR chemical shifts of the acetylenic carbon atoms.⁷ Similar correlations have been noted also for the analogous titanocene^{8,9} and hafnocene compounds.¹⁰ Some deviations from a monotonic trend observed for the first reduction potentials^{4,11} were ascribed to a variation of cyclopentadienyl ring tilt (ϕ), which is related to the energy gap between the 1a₁ and b₂ frontier molecular orbitals.¹² Apparently, steric and electronic effects operate simultaneously and, hence, a knowledge of both physicochemical and structural¹³ data is vital

* To whom correspondence should be addressed. E-mail: mach@jh-inst.cas.cz.

[†] Academy of Sciences of the Czech Republic.

[‡] Charles University.

(1) (a) Brintzinger, H.-H.; Fischer, D.; Mühlhaupt, R.; Rieger, B.; Waymouth, R. *Angew. Chem., Int. Ed. Engl.* **1995**, *34*, 1143–1170. (b) Bochmann, M. *J. Chem. Soc., Dalton Trans.* **1996**, 255–270. (c) Mashima, K.; Nakayama, Y.; Nakamura, A. *Adv. Polym. Sci.* **1997**, *133*, 1–51. (d) McKnight, A. L.; Waymouth, R. M. *Chem. Rev.* **1998**, *98*, 2587–2598 (constrained geometry polymerization catalysts). (e) Alt, H. G.; Köppl, A. *Chem. Rev.* **2000**, *100*, 1205–1221. (f) Chen, E. Y.-X.; Marks, T. J. *Chem. Rev.* **2000**, *100*, 1391–1434. (g) Coates, G. W. *J. Chem. Soc., Dalton Trans.* **2002**, 467–475.

(2) (a) Rosenthal, U.; Burlakov, V. V. In *Titanium and Zirconium in Organic Synthesis*; Marek, I., Ed.; Wiley-VCH: Weinheim, Germany, 2002; Chapter 10, pp 355–389. (b) Zr: Negishi, E. I.; Takahashi, T. *Acc. Chem. Res.* **1994**, *27*, 124–130 and references therein. (c) Horton, A. D. *J. Chem. Soc., Chem. Commun.* **1992**, 185–187. (d) Hf: Yoshida, M.; Jordan, R. F. *Organometallics* **1997**, *16*, 4508–4510. (e) Ti: Akita, M.; Yasuda, H.; Nakamura, A. *Bull. Chem. Soc. Jpn.* **1984**, *57*, 480–487. (f) Knight, K. S.; Waymouth, R. M. *Organometallics* **1994**, *13*, 2575–2577. (g) Varga, V.; Petrusová, L.; Čejka, J.; Mach, K. *J. Organomet. Chem.* **1997**, *532*, 251–259. (h) Horáček, M.; Císařová, L.; Karban, J.; Petrusová, L.; Mach, K. *J. Organomet. Chem.* **1999**, *577*, 103–112. (i) Štěpnička, P.; Gyepes, R.; Císařová, L.; Horáček, M.; Kubišta, J.; Mach, K. *Organometallics* **1999**, *18*, 4869–4880.

(3) (a) Möhring, P. C.; Coville, N. J. *J. Organomet. Chem.* **1994**, *479*, 1–29. (b) Möhring, P. C.; Coville, N. J. *J. Mol. Catal.* **1992**, *77*, 41–50. (c) Gassman, P. G.; Callstrom, M. R. *J. Am. Chem. Soc.* **1987**, *109*, 7875–7876. (d) Mansel, S.; Rief, U.; Prosenč, M.-H.; Kirsten, R.; Brintzinger, H.-H. *J. Organomet. Chem.* **1996**, *512*, 225–236 and references therein. (e) Okuda, J. *Top. Curr. Chem.* **1991**, *160*, 99–145.

(4) Langmaier, J.; Samec, Z.; Varga, V.; Horáček, M.; Choukroun, R.; Mach, K. *J. Organomet. Chem.* **1999**, *584*, 323–328.

(5) Gassman, P. G.; Macomber, D. W.; Hershberger, J. W. *Organometallics* **1983**, *2*, 1470–1472.

(6) Bühl, M.; Hopp, G.; von Philipsborn, W.; Beck, S.; Prosenč, M.-H.; Rief, U.; Brintzinger, H.-H. *Organometallics* **1996**, *15*, 778–785.

(7) Hiller, J.; Thewalt, U.; Poláček, M.; Petrusová, L.; Varga, V.; Sedmera, P.; Mach, K. *Organometallics* **1996**, *15*, 3752–3759.

(8) (a) Gassman, P. G.; Campbell, W. H.; Macomber, D. W. *Organometallics* **1984**, *3*, 385–387. (b) Hafner, A.; Okuda, J. *Organometallics* **1993**, *12*, 949–950.

(9) (a) Vondrák, T.; Mach, K.; Varga, V. *J. Organomet. Chem.* **1989**, *367*, 69–76. (b) Vondrák, T.; Mach, K.; Varga, V. *Organometallics* **1992**, *11*, 2030–2034. (c) Varga, V.; Mach, K.; Poláček, M.; Sedmera, P.; Hiller, J.; Thewalt, U.; Troyanov, S. I. *J. Organomet. Chem.* **1996**, *506*, 241–251.

(10) Gassman, P. G.; Winter, C. H. *Organometallics* **1991**, *10*, 1592–1598.

(11) Langmaier, J.; Samec, Z.; Varga, V.; Horáček, M.; Mach, K. *J. Organomet. Chem.* **1999**, *579*, 348–355.

(12) (a) Lauher, J. W.; Hoffmann, R. *J. Am. Chem. Soc.* **1976**, *98*, 1729–1742. (b) Green, J. C. *Chem. Soc. Rev.* **1998**, 263–271.

(13) ϕ values are available for a number of titanocene,¹⁴ zirconocene,¹⁵ and hafnocene dichlorides.¹⁰

for their reliable evaluation. The role of other substituents is much less understood. One example is the trimethylsilyl group, which is also frequently used as a modifying substituent, since both electron-attracting and electron-donating effects have been experimentally observed depending on the property followed.^{10,16–18}

Substituent properties become particularly important in the case of reactive and low-valent early-transition-metal metallocene complexes. A number of titanocene dichlorides [TiCl₂(η⁵-C₅Me₄R)₂] with bulky group R (e.g., benzyl,¹¹ Ph,^{19b} SiR₃^{19a}) have been reduced to the respective electron-deficient titanocenes (14 valence electrons), which either were thermally stable (for SiMe₂-*t*-Bu,^{20a} SiMe₃,^{20b} SiMe₂Ph, SiMePh₂, and SiMe₂-CH₂CH₂Ph^{20c}), stabilized by π-back-bonding coordination to alkynes, advantageously to bis(trimethylsilyl)-ethyne (btmse),^{2a,20b,21} or spontaneously rearranged to more stable Ti^{III} or Ti^{IV} products having a higher number of valence electrons.²² Among them, the trimethylsilyl-substituted complexes are of particular interest because of the low stability of their η²-btmse complexes and easy thermolysis of the latter to stable titanocenes^{20b} as well as the facile activation of one C–H bond at the trimethylsilyl group upon magnesium reduction without added btmse.^{22a} Rather surprisingly, no cyclopentadienyl ligands more bulky than pentamethylcyclopentadienyl have been used in zirconocene chemistry, though various potentially interesting substituent effects were observed.²³ For instance, an introduction of the trimethylsilyl group into [ZrHCl(η⁵-

C₅H₅)₂]_n (Schwartz's reagent)²⁴ or [ZrH(CH₂PPh₂)(η⁵-C₅H₅)₂]_n²⁵ resulted in an increased solubility and performance of these hydrozirconation reagents.²⁶ Steric demands also influence the association of zirconocene hydrides, which are usually obtained from zirconocene dichloride by reaction with borohydride and aluminohydride reagents²⁷ and alkali-metal alkyls²⁸ or by hydrogenolysis of zirconocene dimethyl complexes:²⁹ hydrides with low-substituted cyclopentadienyl ligands form bis(μ-hydrido) dimers,^{27,29a,c,e} whereas [ZrH₂(η⁵-C₅-Me₅)₂]^{29b,30} and other highly substituted zirconocene hydrides^{28,29b,d} remain monomeric. The *ansa*-zirconocene hydrides form always dimeric structures.^{27e,f,29c,e}

In this work, the reduction of [ZrCl₂{η⁵-C₅Me₄-(SiMe₃)₂}]₂ with magnesium in the absence and the presence of btmse and structures of the products are reported and discussed in relation to the known behavior of their titanocene counterparts.

Results and Discussion

The complex [ZrCl₂{η⁵-C₅Me₄(SiMe₃)₂}]₂ (**1**) was obtained by refluxing the respective lithium cyclopentadienide^{19a} with 0.5 molar equiv of ZrCl₄ according to the procedure described for the preparation of [ZrCl₂(η⁵-C₅-Me₅)₂]_{30a} and other highly substituted zirconocene dichlorides.^{30b,c} Yellow crystalline **1** was dissolved in THF containing activated magnesium in large (ca. 4-fold) molar excess, and the mixture was heated to 60 °C until the solution turned intense brown (2–3 days). Crystallization of the reaction mixture afforded the readily hexane soluble compound **2** (isolated yield 25%), a mixture of poorly hexane soluble compounds **3** and **4** in a combined yield of 65%, and a trace amount of **6** (Scheme 1). Complex **2** obviously results from an intramolecular oxidative addition of one Me₂SiCH₂–H bond across the coordinatively unsaturated zirconium center of the plausible zirconocene intermediate which results from the reductive removal of the chloride ligands. The structure of **2** was determined by ¹H and ¹³C NMR spectroscopy

(14) (a) Clearfield, A.; Warner, D. K.; Saldarriaga-Molina, C. H.; Ropal, R.; Bernal, I. *Can. J. Chem.* **1975**, *53*, 1622–1629. (b) McKenzie, T. C.; Sanner, R. D.; Bercaw, J. E. *J. Organomet. Chem.* **1975**, *102*, 457–466. (c) Troyanov, S. I.; Rybakov, V. B.; Thewalt, U.; Varga, V.; Mach, K. *J. Organomet. Chem.* **1993**, *447*, 221–225.

(15) (a) Prout, K.; Cameron, T. S.; Forster, R. A.; Critchley, S. R.; Denton, B.; Rees, G. V. *Acta Crystallogr., Sect. B* **1974**, *30*, 2290–2304. (b) Janiak, C.; Versteeg, U.; Lange, K. H. C.; Weimann, R.; Hahn, E. *J. Organomet. Chem.* **1995**, *501*, 219–234.

(16) (a) Lappert, M. F.; Pickett, C. J.; Riley, P. I.; Yarrow, P. I. *W. J. Chem. Soc., Dalton Trans.* **1981**, 805–813. (b) Antiñolo, A.; Bristow, G. S.; Campbell, G. K.; Duff, A. W.; Hitchcock, P. B.; Kamarudin, R. A.; Lappert, M. F.; Norton, R. J.; Sarjudeen, N.; Winterborn, D. J. W.; Atwood, J. L.; Hunter, W. E.; Zhang, H. *Polyhedron* **1989**, *8*, 1601–1606.

(17) (a) Antiñolo, A.; Lappert, M. F.; Singh, A.; Winterborn, D. W.; Engelhardt, L. M.; Raston, C. L.; White, A. H.; Carty, A. J.; Taylor, N. J. *J. Chem. Soc., Dalton Trans.* **1987**, 1463–1472. (b) Hitchcock, P. B.; Lappert, M. F.; Lawless, G. A.; Olivier, H.; Ryan, E. J. *J. Chem. Soc., Chem. Commun.* **1992**, 474–476. (c) Choukroun, R.; Dahan, F. *Organometallics* **1994**, *13*, 2097–2100.

(18) Gassman, P. G.; Deck, P. A.; Winter, C. H.; Dobbs, D. A.; Cao, D. H. *Organometallics* **1992**, *11*, 959–960.

(19) (a) Horáček, M.; Gyepes, R.; Cisařová, I.; Polášek, M.; Varga, V.; Mach, K. *Collect. Czech. Chem. Commun.* **1996**, *61*, 1307–1320. (b) Horáček, M.; Polášek, M.; Kupfer, V.; Thewalt, U.; Mach, K. *Collect. Czech. Chem. Commun.* **1999**, *64*, 61–72.

(20) (a) Hitchcock, P. B.; Kerton, F. M.; Lawless, G. A. *J. Am. Chem. Soc.* **1998**, *120*, 10264–10265. (b) Horáček, M.; Kupfer, V.; Thewalt, U.; Štěpnička, P.; Polášek, M.; Mach, K. *Organometallics* **1999**, *18*, 3572–3578. (c) Lukešová, L.; Horáček, M.; Štěpnička, P.; Fejfarová, K.; Gyepes, R.; Cisařová, I.; Kubišta, J.; Mach, K. *J. Organomet. Chem.* **2002**, *659*, 186–196.

(21) (a) Rosenthal, U.; Pellny, P.-M.; Kirchbauer, F. G.; Burlakov, V. V. *Acc. Chem. Res.* **2000**, *33*, 119–129. (b) Štěpnička, P.; Gyepes, R.; Cisařová, I.; Horáček, M.; Kubišta, J.; Mach, K. *Organometallics* **1999**, *18*, 4869–4880.

(22) R = SiMe₃: (a) Horáček, M.; Hiller, J.; Thewalt, U.; Polášek, M.; Mach, K. *Organometallics* **1997**, *16*, 4185–4191. R = Ph: (b) Kupfer, V.; Thewalt, U.; Horáček, M.; Petrusová, L.; Mach, K. *Inorg. Chem. Commun.* **1999**, *2*, 540–544. R = benzyl: (c) Kupfer, V.; Thewalt, U.; Tišlerová, I.; Štěpnička, P.; Gyepes, R.; Kubišta, J.; Horáček, M.; Mach, K. *J. Organomet. Chem.* **2001**, *620*, 39–50.

(23) Ryan, E. J. In *Comprehensive Organometallic Chemistry*; Abel, E. W., Stone, F. G. A., Wilkinson, G., Eds.; Elsevier Science: Oxford, U.K., 1995; Vol. 4, Chapter 9, pp 483–499.

(24) (a) Kautzner, B.; Wailes, P. C.; Weigold, H. *J. Chem. Soc., Chem. Commun.* **1969**, 1105. (b) Schwartz, J. *Pure Appl. Chem.* **1980**, *52*, 733–740.

(25) Raoult, Y.; Choukroun, R.; Blandy, C. *Organometallics* **1992**, *11*, 2443–2446.

(26) Erker, G.; Schlund, R.; Krüger, C. *Organometallics* **1989**, *8*, 2349–2355. (b) Raoult, Y.; Choukroun, R.; Basso-Bert, M.; Gervais, D. *J. Mol. Catal.* **1992**, *72*, 47–58.

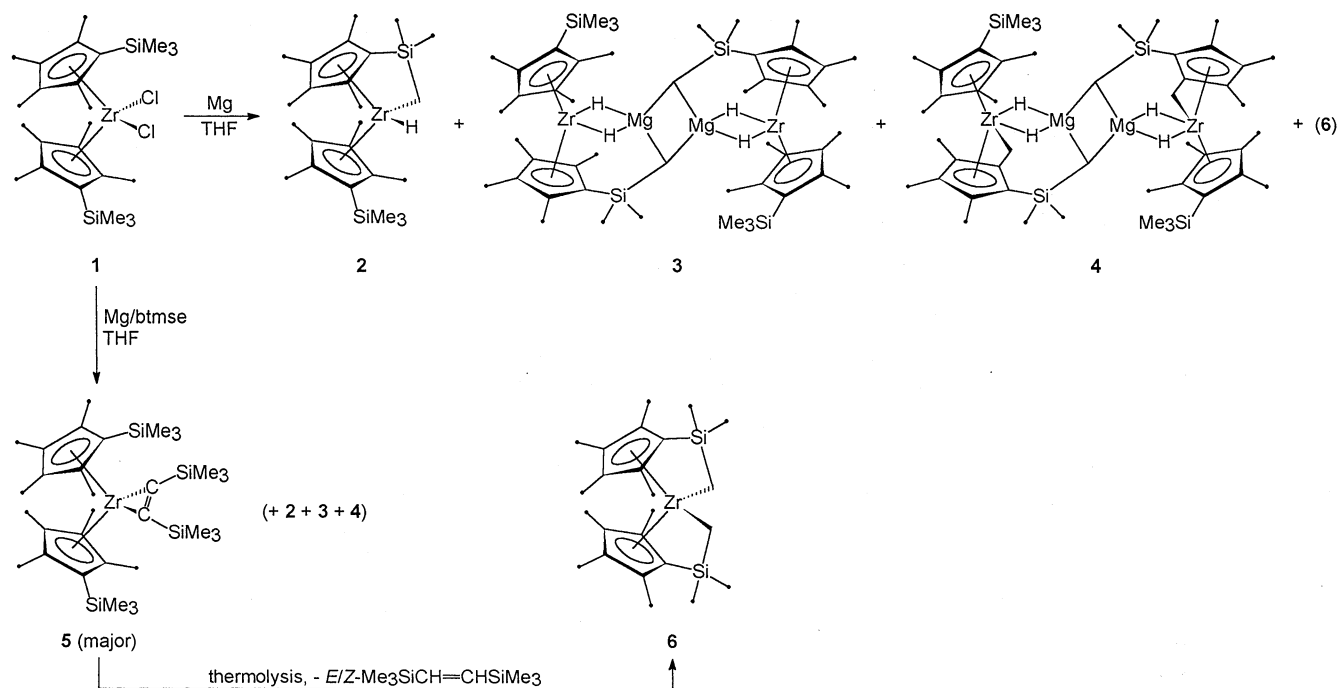
(27) (a) Petersen, J. L.; Jones, S. B. *Inorg. Chem.* **1981**, *20*, 2889–2894. (b) Petersen, J. L.; Jones, S. B. *Organometallics* **1985**, *4*, 966–971. (c) Choukroun, R.; Dahan, F.; Larssonneur, A.-M.; Samuel, E.; Petersen, J. L.; Meunier, P.; Sornay, C. *Organometallics* **1991**, *10*, 374–376. (d) Larssonneur, A.-M.; Choukroun, R.; Jaud, J. *Organometallics* **1993**, *12*, 3216–3224. (e) Reddy, K. P.; Petersen, J. L. *Organometallics* **1989**, *8*, 547–549. (f) Cuenca, T.; Galakhov, M.; Royo, E.; Royo, P. *J. Organomet. Chem.* **1996**, *515*, 33–36. (g) Grossman, R. B.; Doyle, R. A.; Buchwald, S. L. *Organometallics* **1991**, *10*, 1501–1505.

(28) (a) Soleil, F.; Choukroun, R. *J. Am. Chem. Soc.* **1997**, *119*, 2938–2939. (b) Pool, J. A.; Bradley, C. A.; Chirik, P. J. *Organometallics* **2002**, *21*, 1271–1277.

(29) (a) Couturier, S.; Gautheron, B. *J. Organomet. Chem.* **1978**, *157*, C61–C63. (b) Schock, L. E.; Marks, T. J. *J. Am. Chem. Soc.* **1988**, *110*, 7701–7715. (c) Lee, H.; Desrosiers, P. J.; Guzei, I.; Rheingold, A. L.; Parkin, G. *J. Am. Chem. Soc.* **1998**, *120*, 3255–3256. (d) Chirik, P. J.; Day, M. W.; Bercaw, J. E. *Organometallics* **1999**, *18*, 1873–1881. (e) Chirik, P. J.; Henling, L. M.; Bercaw, J. E. *Organometallics* **2001**, *20*, 534–544.

(30) (a) Manriquez, J. M.; Bercaw, J. E. *J. Am. Chem. Soc.* **1974**, *96*, 6229–6230. (b) Manriquez, J. M.; McAlister, D. R.; Sanner, R. D.; Bercaw, J. E. *J. Am. Chem. Soc.* **1978**, *100*, 2716–2724. (c) Courtot, P.; Pichon, R.; Salaun, J. Y.; Toupet, L. *Can. J. Chem.* **1991**, *69*, 127–137.

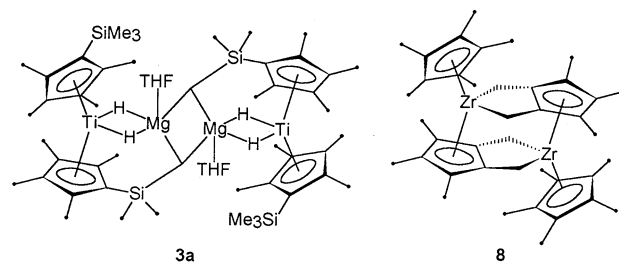
Scheme 1



and further corroborated by single-crystal X-ray diffraction analysis (see below). In the COSY spectrum of **2**, there is observed a cross-peak between ZrH and one of the ZrCH₂ hydrogen atoms ($\delta_{\text{H}} -3.88 \leftrightarrow 5.87$). The structure, however, becomes more apparent from a related COSY spectrum, which in addition to cross-signals due to interactions among the cyclopentadienyl methyl groups and methyls of the SiMe₂ moiety shows interactions between the hydride hydrogen atom and both signals due to ZrCH₂ protons ($\delta_{\text{H}} 5.87 \leftrightarrow -3.88$, ca. 0.41) as well as some of the cyclopentadienyl methyl resonances (namely those at $\delta_{\text{H}} 2.53$ and 1.92 and also weakly with $\delta_{\text{H}} 1.66$ and 1.53). In ¹³C NMR spectra, the signal of ZrCH₂ appears at $\delta_{\text{C}} 42.1$, while all other resonances are found within the expected regions. The stabilization of a transient zirconocene by hydrogen abstraction from the SiMe₃ group by the metal is also reflected in the EI-MS spectrum of **2**, showing the molecular ion (*m/z* 476) as the base peak.

Compounds **3** and **4** could not be separated from each other by fractional crystallization. Nevertheless, the EPR spectra of the mixture in toluene solution and glass (-140 °C) could be unequivocally assigned to the zirconocene (Zr^{III})-magnesium hydride moiety L_nMg(μ-H)₂Zr{η⁵-C₅Me₄(SiMe₃)₂. The triplet 1:2:1 splitting due to a coupling of the Zr(III) d¹ electron with two equivalent bridging hydride ligands (*a*_H = 7.1 G at *g* = 1.9870) resembles the EPR response of similar titanocene (Ti^{III})-magnesium hydride complexes [Ti(μ-H)₂Mg(OEt₂)₂] (*n* = 0–5) (*g* = 1.9911–1.9934, *a*_H = 6.6–7.5 G).³¹ An analogous reduction of [TiCl₂{η⁵-C₅-Me₄(SiMe₃)₂] with magnesium metal gave the titanocene (Ti^{III})-magnesium hydride dimer **3a** (Chart 1), whose trimethylsilyl groups underwent an activation to give two methylene groups ligating two magnesium

Chart 1



atoms in electron-deficient three-centered Mg–C–Mg bonds. This bonding mode of magnesium atoms was not reflected in the EPR spectrum of **3a**, which exhibits triplet splitting with *a*_H = 7.4 G at *g* = 1.9905.^{22a} Our suggestion that compound **3** possesses a structure analogous to **3a** has been corroborated by the crystal structure of **4**, which shows the same bridging mode between the magnesium atoms using the silylmethylene groups as does **3a** and differs only by the presence of one methylene group in the vicinity of the activated trimethylsilyl substituent and the absence of coordinated THF. The methylene group in **4** is σ-bonded³² to zirconium and thus increases the valency of the metal to 4. The absence of THF in both compounds **3** and **4** was further proved by the absence of a THF ion (*m/z* 72) in EI-MS spectra of the **3–4** mixture. The reason for the absence of coordinated THF in **4** can be found in the higher steric congestion at the Mg atoms resulting from longer Zr–cyclopentadienyl ring distances compared to those in **3a**.^{22a} The elemental analysis of the mixture of **3** and **4** cannot assess the abundance of the components, because the compounds differ from each other by only two hydrogen atoms. The ESCA analysis of the mixture, however, gave a molar ratio Si:Zr:Mg

(31) (a) Troyanov, S. I.; Varga, V.; Mach, K. *J. Organomet. Chem.* **1993**, *461*, 85–90. (b) Brintzinger, H. H. *J. Am. Chem. Soc.* **1967**, *89*, 6871–6877.

(32) The presence of a d¹ electron in the single tucked-in permethyltitanocene complex [Ti{η⁵-η¹-C₅Me₄(CH₂)}(η⁵-C₅Me₅)] was proved by UV-photoelectron spectroscopy: Vondrák, T.; Mach, K.; Varga, V.; Terpstra, A. *J. Organomet. Chem.* **1992**, *425*, 27–39.

equal to 2:1.04:0.96 (accuracy $\pm 10\%$), in accordance with the formulation for **3** and **4**. The content of paramagnetic **3** in the **3–4** mixture was estimated from integrated ESR spectra to be 10–20%. Since the ^1H and ^{13}C NMR spectra of the mixture show extremely broadened signals due to the presence of paramagnetic **3**, our assignment of structures **3** and **4** is based mainly on the ESCA and ESR spectra and the crystal structure of **4**.

The reduction of **1** with excess magnesium and in the presence of btmse afforded the green zirconocene complex $[\text{Zr}\{\eta^5\text{-C}_5\text{Me}_4(\text{SiMe}_3)_2(\eta^2\text{-btmse})\}]$ (**5**) as the major product, which was separated and characterized by ^1H and ^{13}C NMR, EI MS, and UV–vis spectra and X-ray single-crystal diffraction. The minor byproducts were complex **2**, which was isolated and identified by ^1H and ^{13}C NMR spectra, and, as revealed by ESR, IR, and ESCA spectra, also complexes **3** and **4**. The resonance of acetylenic carbon atoms in **5** at δ_{C} 259.5 falls within the range observed for the series of $[\text{Zr}(\eta^5\text{-C}_5\text{H}_5\text{-}_n\text{Me}_n)_2(\eta^2\text{-btmse})]$ ($n = 2\text{--}5$) compounds ($n = 2$, δ_{C} 258.2; $n = 5$, δ_{C} 260.5).⁷ The EI-MS spectra of **5** show only the ions due to $[\text{Zr}\{\eta^5\text{-C}_5\text{Me}_4(\text{SiMe}_3)_2\}]^{2+}$ and btmse^{2+} and fragment ions of the latter. The electronic absorption spectrum of **5** in the visible region exhibits a band at 740 nm, which fits among the values found for $[\text{Zr}(\eta^5\text{-C}_5\text{H}_2\text{Me}_3)_2(\eta^2\text{-btmse})]$ (745 nm) and $[\text{Zr}(\eta^5\text{-C}_5\text{HMe}_4)_2(\eta^2\text{-btmse})]$ (738 nm), the fully methylated complex showing the band at 725 nm.⁷ On the other hand, the $\nu(\text{C}\equiv\text{C})$ vibration of **5** is shifted to 1500 cm^{-1} —a value still lower than that for $[\text{Zr}(\eta^5\text{-C}_5\text{Me}_5)_2(\eta^2\text{-btmse})]$ (1516 cm^{-1}).⁷ This indication of a more strongly bonded btmse was not, however, reflected in the solid-state structures, which show virtually the same geometry for the coordinated alkyne (see below).

Thermolysis of **5** under vacuum (10^{-3} Torr) at $170\text{ }^\circ\text{C}$ afforded mainly $[\text{Zr}\{\eta^5\text{-}\eta^1\text{-C}_5\text{Me}_4(\text{SiMe}_2\text{CH}_2)\}_2]$ (**6**, 65% isolated yield) and a mixture of (*E*)- and (*Z*)- $\text{Me}_3\text{SiCH}=\text{CHSiMe}_3$ (*E* \gg *Z*). The structure of **6** was deduced from ^1H and ^{13}C NMR spectra, which show only one set of resonances due to the $\eta^5\text{-}\eta^1\text{-C}_5\text{Me}_4(\text{SiMe}_2\text{CH}_2)$ ligand at δ values very similar to those for **2**. Furthermore, the structure of **6** was confirmed by X-ray diffraction analysis (see below). The mechanism of complex **6** formation has not been studied, though one may consider that **6** results from a 2-fold hydrogen transfer from peripheral SiMe_3 groups onto the leaving btmse upon thermally induced elimination of the alkyne ligand from **5** to give a reactive zirconocene intermediate. Another very minor product, **7**, was detected in the crude sublimate from pyrolysis by ^1H and ^{13}C NMR spectra. On the basis of these spectra, the compound can be ascribed one of the two structures $[\{\text{Zr}(\mu\text{-H})(\eta^1\text{-}\eta^5\text{-C}_5\text{Me}_4\text{SiMe}_2\text{CH}_2)(\eta^5\text{-C}_5\text{Me}_4(\text{SiMe}_3))\}_2]$ and $[\{\text{ZrH}(\eta^1\text{-}\eta^5\text{-C}_5\text{Me}_4\text{SiMe}_2\text{CH}_2)(\eta^5\text{-C}_5\text{Me}_4(\text{SiMe}_3))\}_2]$.

Crystal Structure of 2. The monoclinic unit cell of **2** contains four molecules (Figure 1 and Table 1). The pseudotetrahedrally coordinated tetravalent zirconium atom in a bent-zirconocene moiety is σ -bonded to one methylene carbon atom (C19), forming a bridge to silicon (Si1), and to one hydrogen atom. The $\text{Zr}\text{--}\text{C}(19)$ and $\text{Zr}\text{--}\text{H}$ bond lengths do not deviate from the usual values; the latter ($1.80(2)\text{ \AA}$) is close to the values for nonbridging hydrides, e.g., $[\{\eta^5\text{-C}_5\text{H}_4\text{Me}\}_2\text{ZrH}(\mu\text{-H})_2]$ ^{27a,c} and

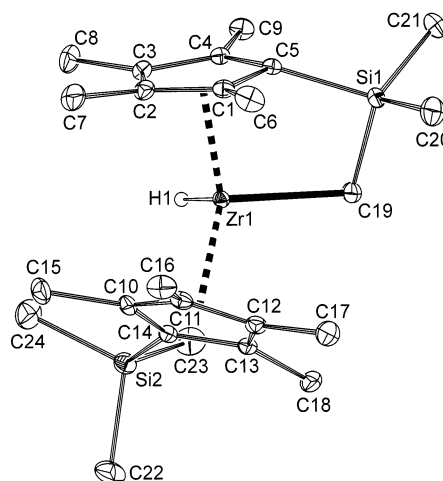


Figure 1. Molecular structure of **2**.

Table 1. Selected Bond Lengths (\AA) and Bond Angles (deg) for **2**

Zr–Cg(1) ^a	2.219(2)	Zr–Cg(2) ^a	2.221(2)
Zr–C(1)	2.500(2)	Zr–C(2)	2.585(2)
Zr–C(3)	2.581(2)	Zr–C(4)	2.502(2)
Zr–C(5)	2.475(2)	Zr–C(19)	2.292(2)
Zr–C(10)	2.499(2)	Zr–C(11)	2.553(2)
Zr–C(12)	2.564(2)	Zr–C(13)	2.534(2)
Zr–C(14)	2.503(2)	Zr–H	1.80(2)
Si(1)–C(19)	1.836(2)	Si(1)–C(5)	1.886(2)
Si(2)–C(14)	1.876(2)	Si–C _{Me}	1.866(2)–1.873(2)
Cg(1)–Zr–Cg(2)	142.8(2)	C(19)–Zr–H	99.8(7)
Zr–C(19)–Si(1)	100.08(9)	C(5)–Si(1)–C(19)	95.11(8)
Cg(1)–Zr–H	99.6(8)	Cg(2)–Zr–H	101.0(8)
Cg(1)–Zr–C(19)	99.4(1)	Cg(2)–Zr–C(19)	107.3(1)
ϕ^b	34.9(1)	ψ^c	13.5(9)
ω^d	22.6(9)	τ^e	113.1(3)

^a Cg(1) and Cg(2) are centroids of the C(1–5) and C(10–14) cyclopentadienyl rings, respectively. ^b Dihedral angle between the least-squares cyclopentadienyl planes. ^c Dihedral angle subtended by the least-squares C(1–5) cyclopentadienyl plane and the $\text{ZrHC}(19)$ plane. ^d Dihedral angle subtended by the least-squares C(10–14) cyclopentadienyl plane and the $\text{ZrHC}(19)$ plane. ^e Torsion angle C(5)–Cg(1)–Cg(2)–C(14).

$[\{\text{Me}_2\text{Si}(\eta^5\text{-C}_5\text{H}_4)_2\text{ZrH}(\mu\text{-H})\}_2]$.^{27e} The Cg(1)–Zr–Cg(2) angle of $142.8(1)^\circ$ and the angle subtended by the least-squares planes of the cyclopentadienyl rings C(1–5) and C(10–14), $\phi = 34.9(1)^\circ$, sum up to $177.6(1)^\circ$, which differs from 180° due to a slight tilting of the C(1–5) plane toward the bridge. As a result, the angle between the “equatorial” plane $\{\text{ZrHC}(19)\}$ and the C(1–5) plane is only $13.5(9)^\circ$, compared to $22.6(9)^\circ$ for the $\{\text{ZrHC}(19)\}$ and C(10–14) planes. Consequently, the Si(1) atom is largely declined from the C(1–5) plane ($0.750(3)\text{ \AA}$) toward the zirconium atom, whereas all the other methyl carbons at the cyclopentadienyl rings and the Si(2) atom deviate in the opposite direction (maximum C(7) $0.226(4)\text{ \AA}$ and C(16) $0.244(4)\text{ \AA}$). On the other hand, bridging of the C(1–5) ring to the zirconium atom has no influence on the Cg–Zr bond distances, which are identical for Cg(1) and Cg(2) within the precision of measurement (2.220 \AA). The dihedral angle C(5)–Cg(1)–Cg(2)–C(14), involving carbon atoms bearing the silyl substituents, is $113.1(2)^\circ$ (see the comparison with the structure of **6** below).

Crystal Structure of 4. The centrosymmetric dimeric molecules of **4** crystallize in the monoclinic space group $P2_1/c$ (Figure 2 and Table 2). One cyclopentadi-

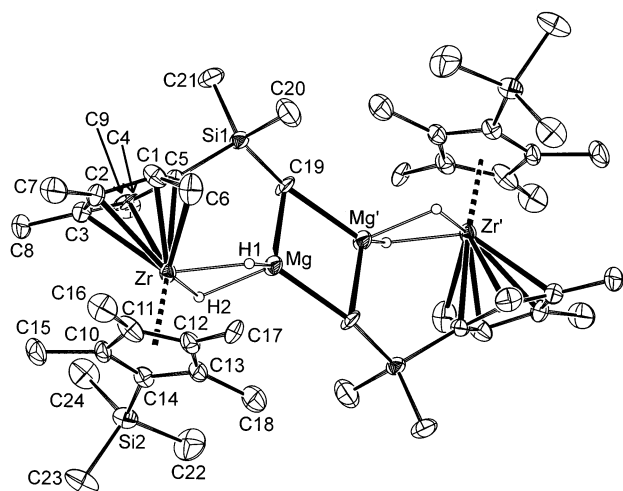


Figure 2. Molecular structure of 4.

Table 2. Selected Bond Lengths (Å) and Bond Angles (deg) for 4

Zr–Cg(1) ^a	2.171(9)	Zr–Cg(2) ^a	2.226(9)
Zr–C(1)	2.297(8)	Zr–C(2)	2.479(11)
Zr–C(3)	2.622(10)	Zr–C(4)	2.598(9)
Zr–C(5)	2.432(8)	Zr–C(6)	2.523(8)
Zr–C(10)	2.537(6)	Zr–C(11)	2.549(7)
Zr–C(12)	2.561(10)	Zr–C(13)	2.503(10)
Zr–C(14)	2.505(7)	Zr–H(1)	1.89(6)
Zr–H(2)	1.92(4)	Mg–H(1)	1.81(5)
Mg–H(2)	1.86(4)	Mg–C(19)	2.218(9)
Mg'–C(19)	2.255(9)	Si(1)–C(19)	1.858(7)
Si(1)–C(5)	1.874(5)	Si(1)–C(20)	1.860(7)
Si(1)–C(21)	1.848(11)	Si(2)–C(14)	1.881(5)
Si(2)–C _{Me}	1.831(13)– 1.870(9)	C(1)–C(6)	1.446(15)
C _{Cp} –C _{Cp} (Cg(1))	1.390(7)– 1.457(8)	C _{Cp} –C _{Me} (Cg(1))	1.506(8)– 1.520(10)
C _{Cp} –C _{Cp} (Cg(2))	1.408(10)– 1.423(12)	C _{Cp} –C _{Me} (Cg(2))	1.485(11)– 1.556(11)
Cg(1)–Zr–Cg(2)	144.0(3)	C(1)–Zr–C(6)	34.5(4)
Zr–C(6)–C(1)	64.1(4)	H(1)–Zr–H(2)	72(2)
H(1)–Mg–H(2)	75(2)	C(19)–Mg–C(19')	104.3(3)
Mg–C(19)–Mg'	75.7(3)	C(5)–Si(1)–C(19)	113.4(3)
Cg(1)–Zr–H(1)	109.6(6)	Cg(1)–Zr–H(2)	99.7(6)
Cg(2)–Zr–H(1)	103.7(6)	Cg(2)–Zr–H(2)	103.2(6)
ϕ^b	32.6(3)	ψ^c	20.8(3)
τ^d	89.3(4)		

^a Cg(1) and Cg(2) are centroids of the C(1–5) and C(10–14) cyclopentadienyl rings, respectively. ^b Dihedral angle between the least-squares cyclopentadienyl planes. ^c Dihedral angle subtended by the H(1)ZrH(2) and H(1)MgH(2) planes. ^d Torsion angle C(5)–Cg(1)–Cg(2)–C(14).

enyl ligand in the assumed zirconocene intermediate remains untouched, while the other is doubly activated by abstraction of hydrogen atoms from the trimethylsilyl and its adjacent methyl group. The methylene groups generated from the trimethylsilyl groups ligate two magnesium atoms in two two-electron–three-center Mg–C–Mg bonds, forming a centrosymmetric rhombohedron with angles C(19)–Mg–C(19)' = 104.3(3)° and Mg–C(19)–Mg' = 75.7(3)°. The zirconium atom is declined slightly away from the rhombohedral plane (0.048(7) Å), and as a consequence, the pairs of Zr–H and Mg–H bond lengths slightly differ (Table 2). The Zr–H bonds are on average shorter than the bridging bonds in dimeric zirconocene dihydrides,^{27a,c,e} while the Mg–H and Mg–C(19) bonds are somewhat shorter than the respective bond lengths in titanocene analogue **3a**

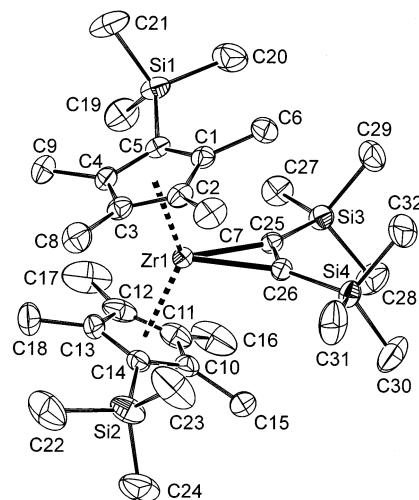


Figure 3. Molecular structure of 5.

Table 3. Selected Bond Lengths (Å) and Bond Angles (deg) for 5

Zr–Cg(1) ^a	2.279(3)	Zr–Cg(2) ^a	2.271(3)
Zr–C(25)	2.228(3)	Zr–C(26)	2.219(3)
Zr–C(1)	2.604(3)	Zr–C(2)	2.585(3)
Zr–C(3)	2.579(4)	Zr–C(4)	2.565(4)
Zr–C(5)	2.564(3)	Zr–C(10)	2.552(4)
Zr–C(11)	2.575(4)	Zr–C(12)	2.567(4)
Zr–C(13)	2.589(4)	Zr–C(14)	2.555(4)
C(25)–C(26)	1.327(5)	Si(1)–C(5)	1.875(4)
Si(2)–C(14)	1.872(4)	Si(3)–C(25)	1.870(4)
Si(4)–C(26)	1.868(4)	Si–C _{Me}	1.834(7)–1.902(7)
Cg(1)–Zr–Cg(2)	139.2(2)	C(25)–Zr–C(26)	34.7(1)
Zr–C(25)–C(26)	72.3(2)	Zr–C(26)–C(25)	73.0(2)
Si(3)–C(25)–C(26)	133.7(3)	Si(4)–C(26)–C(25)	134.4(3)
ϕ^b	41.5(2)	ψ^c	22.4(2)
ω^d	19.4(2)	τ^e	179.4(3)

^a Cg(1) and Cg(2) are centroids of the C(1–5) and C(10–14) cyclopentadienyl rings, respectively. ^b Dihedral angle between the least-squares cyclopentadienyl planes. ^c Dihedral angle subtended by the least-squares C(1–5) cyclopentadienyl plane and the ZrC(25)C(26) plane. ^d Dihedral angle subtended by the least-squares C(10–14) cyclopentadienyl plane and the ZrC(25)C(26) plane. ^e Torsion angle C(5)–Cg(1)–Cg(2)–C(14).

(Chart 1). The planes of the hydride bridges are bent, the dihedral angle between {ZrH(1)H(2)} and {MgH(1)H(2)} planes being 21(3)°, while the rhombohedral plane and the latter planes are nearly perpendicular (dihedral angle 87(2)°). The Zr–Cg(1) (Cg(1) is the centroid of the C(1–5) cyclopentadienyl ring) distance is slightly shorter than Zr–Cg(2) (Cg(2) is the centroid of the C(10–14) ring) (2.171(8) vs 2.226(8) Å). Zr–C(1) (2.297(8) Å) and Zr–C(5) (2.432(8) Å) are the shortest bonds and Zr–C(3) (2.622(10) Å) the longest bond to zirconium in the C(1–5) ring, while the bond to *exo*-methylene, Zr–C(6) (2.523(8) Å) falls within this range. The Si(1) atom is declined from the least-squares plane C(1–5) by 0.485(15) Å outward, and its Si(1)–C(19) bond of 1.858(7) Å falls in the range of the other Si–C bonds in the molecule (1.831(13)–1.881(5) Å). The Mg–Mg' (2.744(3) Å) and Zr–Mg distances (2.953(3) Å) are nonbonding.

Crystal Structure of 5. Complex **5** crystallizes in the monoclinic space group $P2_1/c$ (Figure 3 and Table 3). The geometric parameters of **5** are equal to those found in the crystal structure of [Zr(η^5 -C₅Me₅)₂(η^2 -Me₃-SiC≡CSiMe₃)]⁷ within the precision of measurement,

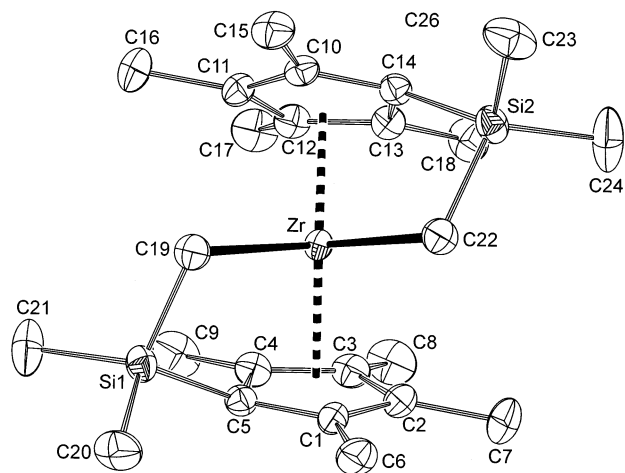


Figure 4. Molecular structure of **6**.

except for the Zr–Cg distances. These are 0.020(5) Å longer in **5**, while the Cg(1)–Zr–Cg(2) and ϕ angles (see Table 3) are virtually the same. The trimethylsilyl groups do not exert any additional steric effect on the zirconocene framework, since they are placed at almost exactly opposite directions with respect to the Cg(1)–ZrCg(2) plane ($\tau = 179.4(3)^\circ$). A comparison with the structure of $[\text{Ti}\{\eta^5\text{-C}_5\text{Me}_4(\text{SiMe}_3)\}_2(\eta^2\text{-Me}_3\text{SiC}\equiv\text{CSiMe}_3)]^{20b}$ shows that the bond lengths Zr–Cg(1) and Zr–Cg(2) as well as Zr–C(25) and Zr–C(26) are about 0.1 Å longer than the corresponding bonds to titanium, which corresponds to a larger covalent radius of Zr (1.45 Å) with respect to Ti (1.32 Å).³³ Nevertheless, a longer bond length between the acetylenic carbon atoms in **5** (C(25)–C(26) = 1.327(5) vs 1.313(4) Å) indicates a stronger binding of btmse, in line with the higher electropositivity of zirconium.

Crystal Structure of 6. The molecule of **6**, symmetrical in solution, is crystallographically unsymmetric in a triclinic crystal (Figure 4). The molecular parameters of two methylene-bridged dimethylsilyl)cyclopentadienylzirconium moieties differ only within the precision of measurement (Table 4) and are very close to the parameters of the same moiety in compound **2** (cf. Table 1). The C(19)ZrC(22) plane is not perpendicular to the Cg(1)ZrCg(2) plane ($84.5(2)^\circ$); however, it subtends virtually the same dihedral angle with both least-squares planes C(1–5) and C(10–14) ($20.0(2)$ and $20.7(2)^\circ$, respectively), whose sum is thus larger than the value of dihedral angle ϕ of $36.9(2)^\circ$. The C(19)–Zr–C(22) angle $98.77(14)^\circ$ does not actually differ from the C(19)–Zr–H angle in **2** ($99.8(7)^\circ$), and the torsion angle C(5)–Cg(1)–Cg(2)–C(14) = $117.5(2)^\circ$ is close to that found in **2** ($113.1(3)^\circ$).

Relation to Titanium Chemistry. A comparison of the products arising from C–H bond activation reactions aided by the central atoms in analogous titanocene and zirconocene systems under similar conditions is now available. Both metals induce an activation process when reduced to a formally divalent state with activated magnesium. The reduction potential of zirconium is about 0.9 V more negative than that of titanium,⁴ and the difference is naturally reflected in the products of C–H bond activation: the easier reducibility of titanium

Table 4. Selected Bond Lengths (Å) and Bond Angles (deg) for **6**

Zr–Cg(1) ^a	2.241(3)	Zr–Cg(2) ^a	2.239(3)
Zr–C(1)	2.526(3)	Zr–C(2)	2.600(3)
Zr–C(3)	2.592(3)	Zr–C(4)	2.513(3)
Zr–C(5)	2.500(3)	Zr–C(19)	2.322(3)
Zr–C(10)	2.528(3)	Zr–C(11)	2.603(3)
Zr–C(12)	2.593(3)	Zr–C(13)	2.506(3)
Zr–C(14)	2.495(3)	Zr–C(22)	2.321(3)
Si(1)–C(19)	1.831(4)	Si(1)–C(5)	1.889(3)
Si(2)–C(22)	1.837(4)	Si(2)–C(14)	1.889(3)
Si–C _{Me}	1.857(5)–1.871(4)		
Cg(1)–Zr–Cg(2)	140.3(1)	C(19)–Zr–C(22)	98.77(14)
Zr–C(19)–Si(1)	100.59(15)	Zr–C(22)–Si(2)	100.38(14)
C(5)–Si(1)–C(19)	95.66(15)	C(14)–Si(2)–C(22)	95.61(15)
ϕ^b	37.0(2)	ψ^c	20.0(2)
ω^d	20.7(2)	τ^e	117.5(2)

^a Cg(1) and Cg(2) are centroids of the C(1–5) and C(10–14) cyclopentadienyl rings, respectively. ^b Dihedral angle between the least-squares cyclopentadienyl planes. ^c Dihedral angle subtended by the least-squares C(1–5) cyclopentadienyl plane and the ZrC(19)C(22) plane. ^d Dihedral angle subtended by the least-squares C(10–14) cyclopentadienyl plane and the ZrC(19)C(22) plane. ^e Torsion angle C(5)–Cg(1)–Cg(2)–C(14).

with respect to zirconium brings about a structure analogous to **2** that is only a reactive intermediate for the titanocene case, the activation being followed by reduction to the Ti(III) complex $[\text{Ti}\{\eta^5\text{-}\eta^1\text{-C}_5\text{Me}_4(\text{SiMe}_2\text{-CH}_2)\}\{\eta^5\text{-C}_5\text{Me}_4(\text{SiMe}_3)\}]$ (**2a**). Although not unequivocally proved, the titanium analogue of compound **3** (see **3a** in Chart 1), a minor byproduct, was proposed to act as the hydrogen acceptor, as it needs to acquire one hydrogen atom per metal center from another source.^{22a} In the zirconium system, compound **3** represents a minor component with respect to **2** and **4**, and the source of its hydrogen still remains unknown. In **4**, the second hydrogen required for the Zr–Mg bridging is likely gained from the intramolecular activation of one C–H bond at the methyl group adjacent to the silyl group, which is likely to be involved in the primary activation reaction. The stabilization of **5** is apparently more efficient than the stabilization of the analogous titanocene complex $[\text{Ti}\{\eta^5\text{-C}_5\text{Me}_4(\text{SiMe}_3)\}_2(\eta^2\text{-btmse})]$ (**5a**), because the latter is not formed under similar conditions (reaction temperature 60 °C). To obtain **5a**, the respective titanocene dichloride was first reduced to the monochloride complex and the subsequent reduction to **5a** was carried out at –18 °C to prevent subsequent reactions.^{20b} A similar lowering of reaction temperature aimed at obtaining pure **5** met with no success, since the reduction of **1** proceeded very slowly if at all. At 60 °C, however, byproducts **2–4** always formed, even in the presence of excess btmse. In contrast to the low thermal stability of **5a**, which liberates btmse at only 80 °C to give the stable titanocene $[\text{Ti}\{\eta^5\text{-C}_5\text{Me}_4(\text{SiMe}_3)\}_2]$,^{20b} compound **5** is thermally very stable, thermolyzing at 170 °C to yield mainly **6** with liberation of isomeric 1,2-bis(trimethylsilyl)ethenes. The very minor byproduct **7**, observed in NMR spectra of the crude product, is probably a dimer bound by methylene bridges between silicon and zirconium atoms. The dimerization of fully methylated zirconocene via two vicinal bridging methylene groups and the crystal structure of the dimer $[\{\mu\text{-}1\eta^5\text{:}2\eta^1\text{:}2\eta^1\text{-C}_5\text{Me}_3(\text{CH}_2)_2\}\{\mu\text{-}$

(33) Pauling, L. *The Nature of the Chemical Bond*, 3rd ed.; Cornell University Press: Ithaca, NY, 1960; p 403.

$2\eta^5:1\eta^1:1\eta^1\text{-C}_5\text{Me}_3(\text{CH}_2)_2\{\text{Zr}(\eta^5\text{-C}_5\text{Me}_5)\}_2\}$ (**8**) (see Chart 1) were reported by Teuben et al.³⁴

Experimental Section

General Considerations. All reductions and operations with reduced zirconium complexes were carried out under vacuum in all-sealed glass devices equipped with breakable seals. Ultraviolet–near-infrared (UV–near-IR) and ESR measurements were performed in attached quartz cuvettes (10.0, 1.0 mm, Hellma) and a quartz ESR sample tube. UV–vis spectra were collected on a Varian Cary 17D spectrometer in the 300–2000 nm range. ESR spectra were measured on an ERS-220 spectrometer (Centre for Production of Scientific Instruments, Academy of Sciences of GDR, Berlin, Germany) operated by a CU-1 unit (Magnettech, Berlin, Germany) in the X-band. *g* Values were determined using a Mn²⁺ standard at *g* = 1.9860 (*M*₁ = −1/2 line). An STT-3 variable-temperature unit was used for measurements in the range −143 to +23 °C. A double integration of isotropic spectra of the **3–4** sample and that of the standard [$(\eta^5\text{-C}_5\text{H}_5)_2\text{Ti}(\mu\text{-Cl})_2\text{AlClEt}$], 5.27×10^{-3} M in benzene) was used to estimate the content of **3**. EI-MS spectra were obtained on a VG-7070E double-focusing mass spectrometer at 70 eV. The crystalline samples in sealed capillaries were opened and inserted into the direct inlet under argon. The spectra are represented by the peaks of relative abundance higher than 7% and by important peaks of lower intensity. X-ray photoelectron spectra (XPS) were measured with a Gammadata Scienta ESCA 310 electron spectrometer using monochromatized Al K α radiation for electron excitation ($\lambda = 1486.6$ eV). The spectra of Mg 2s, Si 2p, Zr 3d, and C 1s electrons were measured. Photoelectron peak areas were calculated after removal of Shirley background using corrections for the pertinent photoionization cross-sections and electron analyzer transmission function and accounting for the dependence of the electron inelastic mean free paths on their kinetic energy. A fine crystalline sample of **3** and **4** was fixed using a double-sided sticky tape (Scotch), which precluded the determination of carbon content. The values of bonding energies of Mg 2s and Zr 3d electrons point to the presence of oxides, which is in line with exposure of the sample to air for about 2 min. The adjustment of single crystals into capillaries for X-ray analysis and preparation of KBr pellets for infrared measurements were performed under purified nitrogen in a glovebox (mBraun Labmaster 130, O₂ and H₂O concentrations lower than 2.0 ppm). IR spectra of KBr pellets were recorded in an air-protecting cuvette on a Nicolet Avatar FTIR spectrometer in the range of 400–4000 cm^{−1}.

Chemicals. The solvents THF, hexane, toluene, and benzene-*d*₆ were dried by refluxing over LiAlH₄ and stored as solutions of dimeric titanocene ($(\eta^5:1\eta^5\text{-C}_{10}\text{H}_8)(\mu\text{-H})_2\{\text{Ti}(\eta^5\text{-C}_5\text{H}_5)\}_2$).³⁵ Bis-(trimethylsilyl)ethyne (Fluka) was degassed, stored as a solution of dimeric titanocene for 4 h, and distributed into ampules by distillation. Magnesium turnings (Aldrich, purum for Grignard reactions) were weighed and evacuated. Tetramethyl(trimethylsilyl)cyclopentadiene was synthesized as previously reported.^{19a} Solid ZrCl₄ (Merck) was handled under a nitrogen atmosphere.

Preparation of [ZrCl₂{ $\eta^5\text{-C}_5\text{Me}_4(\text{SiMe}_3)_2$ }]₂ (1**).** Lithium tetramethyl(trimethylsilyl)cyclopentadienide was obtained by adding BuLi in hexane (2.5 M, 32.8 mL, 82 mmol) to the respective cyclopentadiene (15.52 g, 80 mmol) in toluene (500 mL). After the mixture was stirred for 16 h at room temperature, solid ZrCl₄ (8.78 g, 38 mmol; Merck) was added, and this mixture was refluxed for 40 h. The volume of the reaction mixture was reduced by distilling off 250 mL of toluene and,

after cooling to room temperature, 30% aqueous HCl (50 mL) was added. After this mixture was stirred for another 2 h, pale yellow crystals were filtered from a yellow mother liquor and recrystallized from toluene. Yield: 10.4 g (50%), pale yellow crystals.

Mp: 164 °C. ¹H NMR (C₆D₆): δ 0.42 (s, 9 H, SiMe₃), 1.71, 2.15 (2 × s, 6 H, C₅Me₄). ¹³C{¹H} NMR (C₆D₆): δ 2.3 (SiMe₃), 11.7, 15.7 (C₅Me₄); 125.7 (2 C), 126.4 (1 C), 132.8 (2 C) (C_{ipso}, C₅Me₄). EI-MS (150 °C): *m/z* (relative abundance, %) 548 (7), 546 (M⁺; 6), 535 (12), 534 (8), 533 (17), 532 (9), 531 ([M − Me]⁺; 15), 361 (8), 359 (32), 358 (15), 357 (68), 356 (31), 355 (100), 354 (39), 353 ([M − C₅Me₄(SiMe₃)]⁺; 96), 194 (28), 178 (14), 119 (8), 73 ([SiMe₃]⁺; 85). IR (KBr, cm^{−1}): 2965 (vs, b), 2901 (vs, b), 1482 (m), 1447 (m, b), 1405 (m), 1379 (s), 1333 (s), 1248 (s), 1243 (s), 1128 (w), 1023 (s), 991 (vw), 842 (vs, b), 758 (s), 688 (m), 638 (w), 630 (m), 577 (vw), 422 (s). Anal. Calcd for C₂₄H₄₂Cl₂Si₂Zr (548.90): C, 52.52; H, 7.71. Found: C, 52.43; H, 7.66.

Preparation of [ZrH{ $\eta^5:1\eta^1\text{-C}_5\text{Me}_4(\text{SiMe}_2\text{CH}_2)$ }{ $\eta^5\text{-C}_5\text{Me}_4(\text{SiMe}_3)$ }] (2**).** Crystalline **1** (1.1 g, 2 mmol) was dissolved in THF (30 mL), activated Mg turnings (ca. 0.5 g, 20 mmol) were added, and the mixture was heated at 60 °C for 10 h. The obtained pale brown solution was separated from unreacted magnesium and evaporated under vacuum. A brown residue was extracted with hexane to give a pale yellow solution. Concentration and cooling of the solution afforded crystalline **2**, which was separated and recrystallized from hexane. The yield of pale yellow crystals of **2** was 0.6 g (63%).

Mp: 141 °C. ¹H NMR: δ −3.88 (dd, *J*_{HH} = 1.9, ³*J*_{HH} = 12.5 Hz, 1 H, ZrCH₂), 0.35 (s, 3 H, SiMe₂), 0.40 (s, 9 H, 9 H, SiMe₃), ca. 0.41 (m, 1 H, ZrCH₂; overlapped by a very strong singlet due to SiMe₃ group), 0.63 (s, 3 H, SiMe₂), 1.53, 1.55, 1.66, 1.72, 1.80, 1.92, 2.15 (7 × s, 3 H, C₅Me₄); 2.53 (d, *J*_{HH} = 0.8 Hz, 3 H, C₅Me₄), 5.87 (s, 1 H, ZrH). ¹³C{¹H} NMR: δ 2.6 (SiMe₂), 2.7 (SiMe₃), 6.4 (SiMe₂), 10.4, 10.6, 11.6, 12.2, 12.7, 12.9, 15.2, 17.4 (C₅Me₄); 42.1 (Zr−CH₂), 106.5, 114.3, 118.0, 118.6, 121.1, 121.4, 122.6, 124.7, 129.9 (C₅Me₄, C_{ipso}; one signal was not found). EI-MS (140 °C): *m/z* (relative abundance, %) 482 (8), 481 (13), 480 (30), 479 (22), 478 (51), 477 (55), 476 (M⁺; 100), 475 (29), 474 (26), 473 (17), 472 (27), 470 (8), 461 (11), 460 (8), 459 (12), 407 (13), 405 (20), 404 (20), 403 ([M − SiMe₃]⁺; 41), 401 (12), 399 (13), 331 (8), 73 ([SiMe₃]⁺; 18). IR (KBr, cm^{−1}): 2940 (s), 2893 (s), 2723 (w), 1560 (w), 1473 (w), 1447 (m), 1400 (w), 1377 (m), 1337 (m), 1323 (w), 1243 (s), 1120 (m), 1077 (w), 1020 (s), 987 (w), 947 (w), 840 (vs), 753 (s), 687 (m), 667 (w), 633 (m), 513 (m), 460 (m). Anal. Calcd for C₂₄H₄₂Si₂Zr (477.99): C, 60.31; H, 8.86. Found: C, 59.98; H, 8.81.

Preparation of a Mixture of Complexes 3 and 4. The brown residue after separation of **2** in the above experiment was extracted with toluene. The toluene extract was evaporated and the brown residue repeatedly extracted with hexane in order to separate the zirconium products from residual MgCl₂. The last extracted solution was allowed to stand over the extracted solid overnight, and then it was separated and discarded. The residue was dissolved in toluene and crystallized by cooling in the refrigerator. A brown polycrystalline material was separated and recrystallized in the same way. Several crystal fragments selected from crystalline aggregates were subjected to X-ray diffraction analysis. The solid was investigated by ESCA spectroscopy for the Zr/Mg/Si content and was characterized by IR spectra. The ¹H and ¹³C NMR spectra of the C₆D₆ solution revealed only broad lines. The ESR spectrum in toluene solution and glass was compatible with structure **3**, whereas the X-ray diffraction analysis of the selected crystals gave evidence for the presence of diamagnetic complex **4**. The content of **3** was estimated from ESR spectra to be 10–20%.

Data for a mixture **3** and **4** are as follows. EI-MS (200 °C): *m/z* (relative abundance, %) 480 (10), 479 (13), 478 (31), 477 (30), 476 ([Zr{C₅Me₄(SiMe₃)₂}]⁺; 69), 475 (55), 474 (100), 473 (55), 472 (100), 471 (18), 470 (23), 469 (10), 468 (10), 463 (8),

(34) Spek, A. L.; Pattiasina, J. W.; Teuben, J. H., *Z. Kristallogr.* **1996**, *211*, 643–644.

(35) Antropiusová, H.; Dosedlová, A.; Hanuš, V.; Mach, K. *Transition Met. Chem. (London)* **1981**, *6*, 90–93.

Table 5. Crystallographic Data and Data Collection and Structure Refinement Details for Compounds 2 and 4–6^a

	2	4	5	6
chem formula	C ₂₄ H ₄₂ Si ₂ Zr	C ₄₈ H ₄₄ Mg ₂ Si ₄ Zr ₂	C ₃₂ H ₆₀ Si ₄ Zr	C ₂₄ H ₄₀ Si ₂ Zr
mol wt	477.98	1004.58	648.38	475.96
cryst syst	monoclinic	monoclinic	monoclinic	triclinic
space group	<i>P</i> 2 ₁ / <i>n</i> (No. 14)	<i>P</i> 2 ₁ / <i>c</i> (No. 14)	<i>P</i> 2 ₁ / <i>c</i> (No. 14)	<i>P</i> $\bar{1}$ (No. 2)
<i>a</i> (Å)	9.0450(2)	8.832(2)	9.7520(1)	8.5260(2)
<i>b</i> (Å)	19.9540(5)	15.7234(15)	38.3120(7)	10.3590(4)
<i>c</i> (Å)	13.9200(3)	19.580(6)	10.2510(2)	15.5410(7)
α (deg)	90	90	90	83.608(2)
β (deg)	91.009(1)	93.60(3)	106.8030(9)	74.265(2)
γ (deg)	90	90	90	67.520(2)
<i>V</i> (Å ³), <i>Z</i>	2512.0(1), 4	2714(1), 4	3666.4(1), 4	1220.72(8), 2
<i>T</i> (K)	293	293	293	293
<i>D</i> _{calcd} (g mL ⁻¹)	1.264	1.229	1.175	1.295
μ (mm ⁻¹)	0.540	0.524	0.449	0.556
cryst size (mm ³)	0.8 × 0.4 × 0.1	0.3 × 0.3 × 0.2	0.6 × 0.5 × 0.2	0.8 × 0.4 × 0.2
θ _{max} (deg)	30.0	25.0	27.1	27.9
no. of unique diffrns	7233	2289	7689	5761
no. of obsd diffrns	5979	1423	7150	4568
no. of params	412	281	334	269
<i>R</i> (<i>F</i>); <i>R</i> _w (<i>F</i> ²) (all data)	5.10; 7.40	9.61; 8.85	6.36; 14.56	6.85; 13.02
<i>R</i> (<i>F</i>) (<i>I</i> > 2 σ (<i>I</i>))	3.40	3.85	5.89	4.76
GOF (all data)	1.062	1.032	1.150	1.152
$\Delta\rho$ (e Å ⁻³)	0.530; -0.679	0.443; -0.755	1.382; -0.834 ^b	0.820; -0.659

^a Definitions: $R(F) = \sum ||F_o| - |F_c|| / \sum |F_o|$; $R_w(F^2) = [\sum (w(F_o^2 - F_c^2)^2) / \sum w(F_o^2)^2]^{1/2}$; GOF = $[\sum (w(F_o^2 - F_c^2)^2) / (N_{\text{diffns}} - N_{\text{params}})]^{1/2}$. ^b A ghost at 1.0 Å from the silicon atom Si(2).

461 (16), 460 (12), 459 (27), 458 (13), 457 (28), 456 (12), 455 (23), 453 (10), 443 (8), 441 (10), 439 (12), 437 (12), 413 (11), 405 (10), 403 (19), 402 (10), 401 (26), 400 (16), 399 (34), 397 (16), 395 (11), 393 (9), 387 (8), 385 (10), 383 (11), 381 (9), 379 (8), 259 (10), 91 (13), 83 (12), 73 (51). IR (KBr, cm⁻¹): 2953 (s), 2902 (s), 2727 (w), 1450 (m), 1378 (m), 1323 (m), 1245 (s), 1127 (m), 1023 (m), 838 (s), 802 (m), 754 (m), 718 (m), 685 (m), 631 (m). UV/vis (toluene, nm): 650 (sh) < 540 (sh). ESCA analysis (atom/molar fraction): Si/1.00, Mg/0.52, Zr/0.48 ($\pm 10\%$). EPR spectra for **3**: in toluene at 23 °C, *g* = 1.9870, *a*_H = 7.1 G, ΔH = 4.3 G; in toluene at -140 °C, *g*₁ = 2.000, *g*₂ = 1.989, *g*₃ = 1.973, *g*_{av} = 1.987.

Preparation of [Zr(η^5 -C₅Me₄SiMe₃)₂(η^2 -Me₃SiC≡CSiMe₃)] (5). Complex **1** (1.1 g, 2 mmol) was dissolved in a mixture of THF (30 mL) and btmse (4 mL, 18 mmol). Magnesium turnings (0.5 g, 20 mmol) were added, and the mixture was heated to 60 °C for 40 h. A greenish brown solution was separated from excess magnesium and evaporated under vacuum, and a brown residue was extracted into hexane to give a green solution. Concentration and cooling of the solution afforded a yellowish crystalline sediment whose identity with **2** was determined by ¹H and ¹³C NMR spectra. Then, the green mother liquor was concentrated and cooled with dry ice overnight, whereupon all the solution solidified; this solid was then placed in a freezer (-18 °C) for 2 days to separate a solid from a greenish mother liquor. The crystalline solid was dissolved in a minimum amount of hexane and recrystallized by cooling to -18 °C. The yield of green crystals of **5** was 0.51 g (39.5%).

Mp: 153 °C. ¹H NMR (C₆D₆): δ 0.16, 0.20 (2 × s, 9 H, SiMe₃); 1.81, 2.17 (2 × s, 6 H, C₅Me₄). ¹³C{¹H} NMR (C₆D₆): δ 2.8, 4.7 (SiMe₃); 13.0, 16.5 (C₅Me₄); 117.2 (1 C), 126.0 (2 C), 127.7 (2 C) (C₅Me₄); 259.5 (η^2 -C≡C). ²⁹Si NMR (C₆D₆): δ -14.7, -9.5 (SiMe₃). EI-MS (170 °C): *m/z* (relative abundance, %) 480 (11), 479 (8), 478 (22), 477 (21), 476 ([M - btmse]⁺; 39), 475 (10), 474 (11), 472 (9), 403 ([M - btmse - SiMe₃]⁺; 9), 170 ([btmse]⁺; 8), 157 (9), 156 (19), 155 ([btmse - Me]⁺; 100), 120 (8), 73 ([SiMe₃]⁺; 62). IR (KBr, cm⁻¹): 2955 (s), 2900 (s), 2858 (m, sh), 1500 (m), 1451 (w, b), 1377 (w), 1349 (vw), 1325 (m), 1246 (s), 1129 (w), 1085 (vw), 1020 (w), 951 (vw), 844 (vs, b), 755 (m), 684 (w), 657 (vw), 635 (vw), 450 (w). UV/vis (hexane, 25 °C): 740 < 360 (sh) < 315 (sh). Anal. Calcd for C₃₂H₆₀Si₄Zr (648.40): C, 59.28; H, 9.33. Found: C, 59.35; H, 9.37.

The residue after the first extraction with hexane and separation of the green product was repeatedly extracted with hexane to give a brown crystalline product. The product was identified as a mixture of **3** and **4** by IR and ESCA spectra, and the presence of **3** in its toluene solution was proved by ESR spectra (vide supra).

Preparation of [Zr(η^1 : η^5 -C₅Me₄(SiMe₂CH₂))₂] (6). Solid **5** (0.78 g, 1.20 mmol) in a sealed glass ampule was heated to 170 °C on an oil bath. The volatiles were collected in a trap cooled by liquid nitrogen. After the mixture was heated for 2 h, a greenish residue and a nearly colorless solid condensed on an outlet glass tube. The solid sublimate was sealed off from the ampule. The solid product was washed out by a minimum amount of hexane to remove traces of **5**, and a nearly colorless residue was dissolved in 10 mL of hexane. Crystallization by cooling from a concentrated solution afforded nearly colorless crystals of **6**. Yield: 0.37 g (65%). Evaporation of the mother liquor afforded a crystalline material which contained, according to NMR spectra, a minor byproduct (**7**) whose ¹H and ¹³C NMR data were obtained by subtraction from those of **6**. GC-MS analysis of the trap contents revealed that it contained largely btmse (major) and (*E*)- and (*Z*)-1,2-bis(trimethylsilyl)ethenes.^{9c}

Data for **6** are as follows. Mp: 229 °C. ¹H NMR (C₆D₆): δ -2.54, -0.78 (2 × d, ²*J*_{HH} = 12.7 Hz, 1 H, ZrCH₂); 0.39, 0.56 (2 × s, 3 H, SiMe₂); 1.53, 1.68, 1.73, 2.29 (4 × s, 3 H, Me₄C₅). ¹H{¹³C} NMR (C₆D₆): δ 3.7, 5.3 (SiMe₂); 10.8, 11.6, 12.7, 15.4 (Me₄C₅); 20.4 (ZrCH₂), 106.2, 119.9, 120.9, 124.9, 154.4 (Me₄C₅). EI MS (130 °C): *m/z* (relative abundance, %) 479 (8), 478 (25), 477 (21), 476 (54), 475 (41), 474 (M⁺; 100), 473 (51), 472 (89), 471 (13), 470 (17), 461 (9), 459 (15), 457 (14), 455 (11), 413 (10), 401 ([M - SiMe₃]⁺; 12), 399 (15), 397 (9), 395 (8), 219 (17), 131 (13), 73 (18). IR (KBr, cm⁻¹): 2967 (s), 2907 (s), 1478 (w), 1446 (m), 1378 (m), 1350 (w), 1326 (m), 1241 (s), 1123 (w), 1083 (w), 1023 (w), 993 (w), 839 (vs), 820 (s), 809 (s), 791 (s), 753 (m), 731 (w), 682 (w), 668 (s), 639 (m), 511 (w), 461 (s), 439 (m). Anal. Calcd for C₂₄H₄₀Si₂Zr (475.98): C, 60.56; H, 8.47. Found: C, 60.25; H, 8.50.

NMR data for the minor byproduct **7**: ¹H NMR (C₆D₆): δ -1.50, -0.68 (2 × d, ²*J*_{HH} = 12.8 Hz, 1 H, ZrCH₂); 0.34 (s, 9 H, SiMe₃), 0.52, 0.61 (2 × s, 3 H, SiMe₂); 1.63, 1.73 (2 C), 1.74, 1.77, 1.96, 1.99, 2.04 (8 × s, 3 H, C₅Me₄); 4.71 (s, 1 H, ZrH). ¹H{¹³C} NMR (C₆D₆): δ 2.2 (SiMe₃), 2.5, 5.6 (SiMe₂); 10.4

(ZrCH₂), 10.5, 10.6, 11.7 (2 C), 13.2, 14.1, 14.2, 14.6 (Me₄C₅); 108.3, 117.4, 119.2, 119.4, 121.1, 122.7, 124.8, 126.0, 127.2, 130.8 (Me₄C₅).

X-ray Crystallography. Colorless crystals of **2** and **6**, brown crystals of **4**, and green crystals of **5** were inserted into Lindemann glass capillaries in a glovebox, and the capillaries were sealed by flame. The diffraction data for complexes **2**, **5**, and **6** were collected on an Nonius KappaCCD diffractometer (Mo K α radiation, $\lambda = 0.71073 \text{ \AA}$) and analyzed by the HKL program package.³⁶ The data for **4** were collected on an Enraf-Nonius CAD 4-MACH III diffractometer using graphite-monochromated Mo K α radiation, $\theta-2\theta$ scans, and BPB integration. In all cases, the structures were solved by direct methods (SIR97),³⁷ followed by consecutive Fourier syntheses and refined by full-matrix least squares on F^2 (SHELX97).³⁸

Relevant crystallographic data are given in Table 5. In all cases, the non-hydrogen atoms were refined anisotropically. The hydrogen atoms were treated as follows. For **2**, all hydrogen atoms were located on difference electron density

(36) Otwinowski, Z.; Minor, W. HKL Denzo and Scalepack Program Package; Nonius BV, Delft, The Netherlands, 1997. For a reference see: Otwinowski, Z.; Minor, W. *Methods Enzymol.* **1997**, *276*, 307–326.

(37) Altomare, A.; Burla, M. C.; Camalli, M.; Cascarano, G.; Giacovazzo, C.; Guagliardi, A.; Polidori, G. *J. Appl. Crystallogr.* **1994**, *27*, 435–436.

(38) Sheldrick, G. M. SHELXL97: Program for Crystal Structure Refinement from Diffraction Data; University of Göttingen, Göttingen, Germany, 1997.

maps and refined isotropically. For **4**, hydrogen atoms H(1) and H(2) and those linked to C(19) were located on difference electron density maps and refined isotropically; all others were refined in their theoretical positions. For **5**, all hydrogen atoms were included into calculated positions. For **6**, hydrogen atoms at C(19) and C(22) were identified on the difference Fourier map and refined with isotropic thermal motion parameters; all other hydrogen atoms were placed at their theoretical positions.

Acknowledgment. This work was financially supported by the Grant Agency of the Czech Republic (Grant Nos. 203/00/DO37 and 203/99/MO37). The Grant Agency of the Czech Republic also sponsored access to the Cambridge Structure Database (Grant No. 203/02/0436). This investigation is also a part of the long-term research plan of the Faculty of Sciences, Charles University.

Supporting Information Available: Tables of crystallographic data, atomic coordinates, thermal parameters, intramolecular distances and angles, and dihedral angles of least-squares planes and packing diagrams for **2** and **4–6**. This material is available free of charge via the Internet at <http://pubs.acs.org>.

OM020883Y